Int. J. Solids Structures Vol. 29, No. 5, pp. 611–639, 1992
Printed in Great Britain.

0020–7683/92 $5.00 + .00

REFINED BUCKLING AND POSTBUCKLING ANALYSIS OF TWO-DIMENSIONAL DELAMINATIONS—II. RESULTS FOR ANISOTROPIC LAMINATES AND CONCLUSION†

K. C. JANE
BMT International, Inc., 10480 Little Papuxent Parkway, Columbia, MD 21044, U.S.A.

and

W.-L. YIN
School of Civil Engineering, Georgia Institute of Technology, Atlanta, GA 30332, U.S.A.

(*Received* 8 *October* 1990; *in revised form* 14 *June* 1991)

Abstract—The analysis scheme developed in Part I of the paper is implemented to obtain the bifurcation strains of circular delaminated layers and the postbuckling solutions of cross-ply and angle-ply elliptical sublaminates. Reasonably accurate solutions for the membrane forces, the bending and twisting moments and the pointwise energy release rates generally require 33 or more undetermined coefficients. Such refined postbuckling solutions show a variety of features including significant non-uniformity of the in-plane forces and certain boundary effects characterized by concentration of the middle-surface curvatures and the bending moments. The solutions are found to be strongly influenced by ply orientation, lay-up and the aspect ratio of the ellipse. Some implications of the analytical results on the buckling and postbuckling behavior of two-dimensional delamination models are summarized.

1. INTRODUCTION

In recent years extensive analytical and numerical studies have been made on sublaminate buckling and crack growth associated with an interior delamination in a homogeneous or laminated plate. For the simple, one-dimensional model of an across-the-width delamination, exact bifurcation loads and closed-form postbuckling solutions have been obtained, in the context of geometrically non-linear plate theory, for delaminated homogeneous plates (Chai *et al.*, 1981; Simitses *et al.*, 1985; Yin *et al.*, 1986; Kardomateas, 1989) and for delaminated laminates with arbitrary ply configurations (Yin, 1986, 1988). The strain-energy release rate associated with delamination growth has been expressed explicitly in terms of sublaminate membrane forces and bending moments at the delamination front, and the results were found to be in agreement with the corresponding results based on non-linear finite-element analysis and the closure–integral method. Recent studies have taken into account the effects of transverse shear deformation (Kardomateas and Schmueser, 1988; Chen, 1990), which may become important in a thick or strongly anisotropic delaminated sublaminate.

The relative ease with which accurate postbuckling solutions of strip delamination models may be obtained is attributable to the fact that, in the one-dimensional case, the differential equations of von Karman's non-linear plate theory reduce to *linear* ordinary differential equations. Hence the effect of geometrical non-linearity is present only in the boundary conditions and the crack-tip continuity conditions for the axial displacement, but not in the governing differential equations. Furthermore, in the one-dimensional case the non-linear coupling between the in-plane deformation and the transverse deflection degenerates to a particularly simple form, characterized by the presence of a *constant* axial load in the deflection equation. Accurate postbuckling solutions of general two-dimensional delamination models are considerably more difficult to obtain in view of the presence of

† A preliminary version of this paper was presented in AIAA/ASME/ASCE/AHS 30th SDM Conference, Mobile, AL, April, 1989.

non-linear and coupling terms in the governing equations. It may be expected that these terms will significantly affect the postbuckling behavior of the sublaminate and the nature of ensuing delamination growth.

A first step toward a better understanding of two-dimensional delamination problems is achieved through a buckling and postbuckling analysis of an isotropic circular delaminated plate subjected to a radially symmetric in-plane compression. The analysis indicates that, with proper normalization, the non-dimensional radial buckling load of the circular model depends on the normalized delamination radius and thickness according to relations extremely close to the corresponding relations for the normalized axial load of a strip delamination model in terms of the normalized delamination length and thickness (Yin and Fei, 1984). For both strip and circular models, a sharp transition from global buckling of the laminate to local buckling of the thin delaminated layer takes place when the delamination reaches a critical size. Furthermore, the postbuckling deformations of the circular and strip delamination models show the same pattern of evolution, from the initiation of buckling to final collapse, which is unique to each regime of delamination size (subcritical or supercritical) and which is fundamentally different between the two regimes (Yin *et al.*, 1986; Yin and Fei, 1988).

In spite of these similarities, there are also significant and essential differences in the buckling and postbuckling behavior of strip and circular delamination models. Axisymmetric postbuckling solutions of the circular model show pronounced boundary effects, non-uniform distribution of the in-plane forces, and generally catastrophic nature of delamination growth. As shown by the analysis of Part I, these effects are also manifest in the postbuckling response of isotropic, thin-film elliptical delamination models under uniaxial compression in the base plate. It was also shown that an accurate assessment of these effects cannot be achieved by lower-order Rayleigh Ritz postbuckling solutions that have been presented in the existing literature. Solutions of at least the order (5, 4) involving 33 or more undetermined coefficients in the polynomial displacement expansions for an anisotropic elliptical sublaminate, are required to provide reasonably accurate results for the membrane forces, bending and twisting moments, and the global and pointwise energy release rates.

Non-linearity and coupling in the von Karman equations, which produce the previously mentioned effects, are strongly dependent on the anisotropic elastic moduli of the plies constituting the sublaminate and on the orientation and lay-up of the plies. While the analysis of *isotropic* sublaminates in Part I has provided some general features of the buckling and postbuckling behavior of two-dimensional delamination models, an understanding of the combined effects of the various geometrical and material parameters can only be gained from a variety of solutions covering a broad range of parameter values. For example, an exact postbuckling analysis of the one-dimensional strip delamination model with a general laminated structure has indicated the significance of the destabilizing effect of bending-extensional coupling (Yin, 1986). Such effects are not present in two-dimensional symmetric sublaminates, including isotropic and orthotropic sublaminates.

In Part II of this paper, we present postbuckling solutions for anisotropic elliptical laminates with various aspect ratios, using polynomial displacement expansions of the order (5, 4). Although our computer code may handle any uniform in-plane strain loading in the base plate, in the present work we restrict the computation to the case of uniaxial compression in the base plate along the minor axis of the ellipse. This loading case was considered in previous buckling analysis of circular, unidirectional composite laminates (Shivakumar and Whitcomb, 1985) and postbuckling analysis of isotropic and specially orthotropic elliptical sublaminates (Chai and Babcock, 1985). In the present work, we obtain the solutions for cross-ply and 30° and 45° angle-ply elliptical sublaminates under postbuckling strain loads as large as four or five times the bifurcation strain. The sublaminates have symmetric or antisymmetric four-layer lay-ups and the aspect ratio of the ellipse ranges from 1, 2 to 4.

Our results for the force and moment resultants and for the global and pointwise energy release rates show complex patterns of behavior, depending strongly on the orientation and the stacking sequence of the plies in the sublaminate and, to a lesser degree, on the aspect

ratio of the ellipse. These results have direct implications on the initiation and development of delamination growth. The complexity and richness of the present results suggests the need for caution in making predictions or conjuctures concerning the buckling and growth behavior of two-dimensional models based either on analytical and experimental experiences with strip delaminations or on insufficiently refined approximate solutions of two-dimensional sublaminates.

2. BIFURCATION LOAD OF A CIRCULAR, UNIDIRECTIONAL SUBLAMINATE

A general and consistent scheme for polynomial representation of displacement functions associated with the buckling and postbuckling deformation of elliptical sublaminates has been developed in Part I of this paper. In the following analysis, we adopt the notations and definitions introduced in Section 2 of Part I.

We first investigate the bifurcation strain of a circular, unidirectional composite layer disbonded from an infinite base laminate, when the latter is subjected to in-plane strains $-E_0$ and $0.3\ E_0$ along the Y- and X-directions, respectively. The angle α between the material axis of fiber orientation and the compression axis is allowed to vary. This problem has been investigated by Shivakumar and Whitcomb (1985) using both finite-element and Rayleigh–Ritz methods. Their Rayleigh–Ritz solutions were based on a three-term polynomial expansion for the normalized transverse deflection w in terms of the dimensionless co-ordinates x and y:

$$w = (1-x^2-y^2)^2 R(x, y) \tag{1}$$

where

$$R(x, y) = c_1 + c_2 x^2 + c_3 y^2.$$

The results were found to be in close agreement with the finite-element results for small orientation angles but not for large angles (Fig. 1).

We notice that the deflection function expressed by the three-term expansion is symmetric with respect to both X- and Y-axes. Since such symmetry conditions cannot be assumed generally except for specially orthotropic sublaminates with aligned loading, material and geometrical axes, certain deflection modes are suppressed by the assumed symmetry and this has the effect of raising the calculated bifurcation load. It is clear that, at least in the initial postbuckling states, the actual deflection should have central symmetry but not double symmetry with respect to both co-ordinate axes, i.e. one should *only* have

$$w(-x, -y) = w(x, y). \tag{2}$$

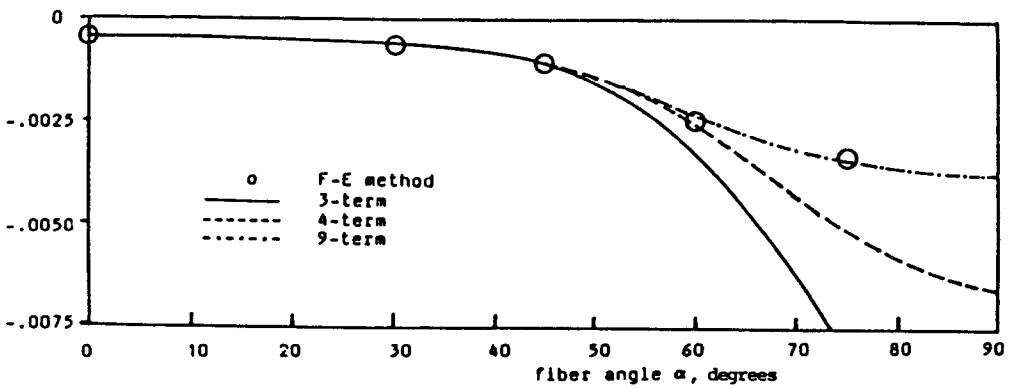

Fig. 1. Bifurcation strain of a circular unidirectional laminate versus the fiber orientation angle.

This implies that, if in eqn (1) one chooses a polynomial factor $R(x, y)$ of degree two, then the factor should include an additional term c_4xy. The new deflection function yields an improved solution for the bifurcation strain (see the middle curve in Fig. 1).

Further improvement in the bifurcation strain may be obtained by including in the polynomial $R(x, y)$ all fourth degree terms that are consistent with the symmetry condition of eqn (2). This yields a nine-term deflection function:

$$w = (1-x^2-y^2)^2(c_1+c_2x^2+c_3xy+c_4y^2+c_5x^4+c_6x^3y+c_7x^2y^2+c_8xy^3+c_9y^4). \tag{3}$$

The resulting bifurcation strains are shown by the top curve in Fig. 1. The results are nearly indistinguishable from the finite-element solutions over the entire range of the orientation angle α. Thus, by including in the polynomial function $P(x, y)$ all fourth and lower degree terms that are consistent with the symmetry condition of eqn (2), the Rayleigh–Ritz analysis yields bifurcation loads that are in excellent agreement with the finite-element solutions.

3. POSTBUCKLING SOLUTIONS OF CROSS-PLY AND ANGLE-PLY ELLIPTICAL SUBLAMINATES

The number of undetermined coefficients required in the Rayleigh–Ritz solutions for the postbuckling deformation is considerably larger. For a general anisotropic elliptical delamination, the normalized postbuckling displacement functions satisfy the following symmetry conditions:

$$u(-x, -y) = -u(x, y), \quad v(-x, -y) = -v(x, y), \quad w(-x, -y) = w(x, y). \tag{4}$$

Hence P and Q (defined in eqn (5) of Part I) are odd polynomials and R is an even polynomial.

The convergence study in Part I for the Rayleigh–Ritz solutions of homogeneous isotropic sublaminates suggests that, in order to obtain reasonably accurate results for the force and moment resultants and the energy release rates, the odd polynomials, P and Q, must include at least terms of the fifth and lower degrees and the even polynomial, R, must include at least terms of the fourth and lower degrees. In this approximation, the polynomials contain a total of 33 undetermined coefficients:

$$\begin{aligned}
P(x, y) &= a_1x+a_2y+a_3x^3+a_4x^2y+a_5xy^2+a_6y^3 \\
&\quad +a_7x^5+a_8x^4y+a_9x^3y^2+a_{10}x^2y^3+a_{11}xy^4+a_{12}y^5, \\
Q(x, y) &= b_1x+b_2y+b_3x^3+b_4x^2y+b_5xy^2+b_6y^3 \\
&\quad +b_7x^5+b_8x^4y+b_9x^3y^2+b_{10}x^2y^3+b_{11}xy^4+b_{12}y^5, \\
R(x, y) &= c_1+c_2x^2+c_3xy+c_4y^2+c_5x^4+c_6x^3y+c_7x^2y^2+c_8xy^3+c_9y^4.
\end{aligned} \tag{5}$$

A further improvement in the solution may be obtained when *all* terms of the next order consistent with the symmetry conditions of eqn (4) are included in the expressions of u, v and w. This will bring the total number of coefficients to 56.

Although higher-order solutions are desirable for improved accuracy, the computer storage and time requirements for evaluating the integrals L_{ij}, M_{ij} and N_{ij} in the potential energy expression (see eqns (6) and (7) of Part I) become increasingly demanding. Besides, since the thin-film assumption itself (i.e. ignoring the effect of layer buckling on the deformation of the thick base plate) may introduce significant error in the results, as has been demonstrated in the cases of strip and circular delamination models (Chai *et al.*, 1981; Yin and Fei, 1988), there is little justification to obtain extremely elaborate postbuckling solutions based on the thin-film approximation. Consequently, the displacement expansions including 33 undetermined coefficients (eqn (14)) are used in the present analysis to obtain postbuckling solutions of four-layer cross-ply, 30° angle-ply and 45° angle-ply elliptical sublaminates with symmetric or anti-symmetric layup (denoted in the figures by S-cross,

U-cross, S30, U30, S45 and U45, respectively). The individual layers are made of T300/5208 graphite epoxy unidirectional composite whose longitudinal elastic modulus E_1 is 17.57 times the transverse elastic modulus E_2 and for which $\nu_{12} = \nu_{21}E_1/E_2 = 0.28$. The aspect ratio of the ellipse, a/b, assumes the values 1, 2 and 4.

The results of a non-linear problem with strong coupling among the dependent variables and involving many geometrical and material parameters cannot be reduced to simple rules of thumb. In this section, an attempt is made to present the large and complex body of postbuckling solutions for various elliptical sublaminates without oversimplification and with a certain degree of consistency and comprehensiveness. As mentioned previously, we restrict the analysis to the loading case when the base plate is subjected to uniform strains 0.3 E_{YY} and $-E_{YY}$ along the X- and Y-directions, respectively.

3.1. *Central deflection*

The central deflection of the delaminated layer in the buckled state is shown in Fig. 2 for the various symmetric and unsymmetric delaminations. Sublaminates with the antisymmetric lay-up buckle at lower compressive strains compared to the corresponding sublaminates with the symmetric lay-up, and the former show larger central deflections, at least in the initial postbuckling states. These results attest to the destabilizing effect caused by the bending–stretching coupling of antisymmetric sublaminates. Figure 2 indicates that, for aspect ratios 2 and 4, the results for the central deflection show similar patterns, while in the case $a/b = 1$ the deflections are generally smaller and the 30° angle-ply sublaminates have the lowest bifurcation strains and the largest postbuckling deflections. This may be explained by the constraining effect provided by the relatively short transverse in-plane axis in the case $a/b = 1$. This constraining effect is less significant for the 30° angle-ply sublaminates because the fibers are largely aligned along the Y-axis and, consequently, the bending stiffness in the X-direction is smaller than in the case of cross-ply and 45° angle-ply sublaminates. Generally, the curves of E_{YY} versus the central deflection show nearly parabolic variations.

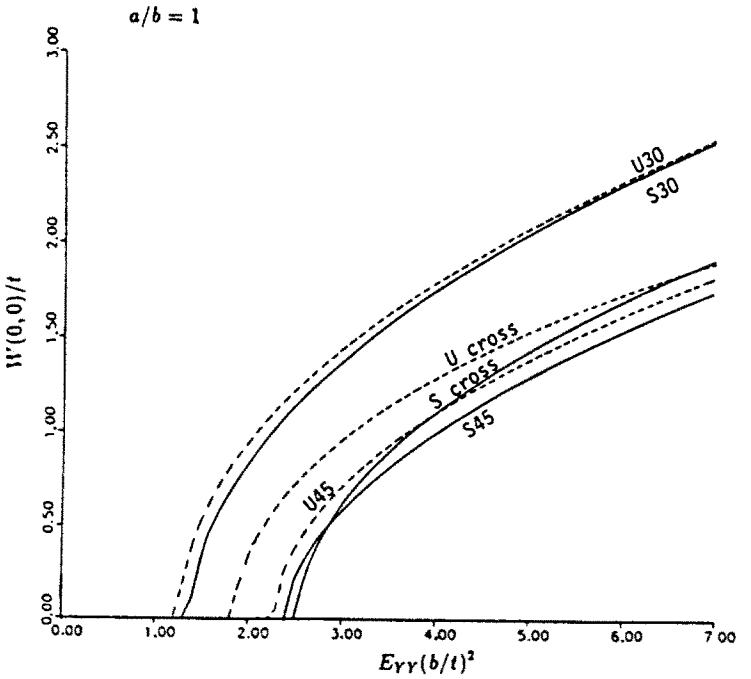

(a)

Fig. 2. Deflection at (0, 0).

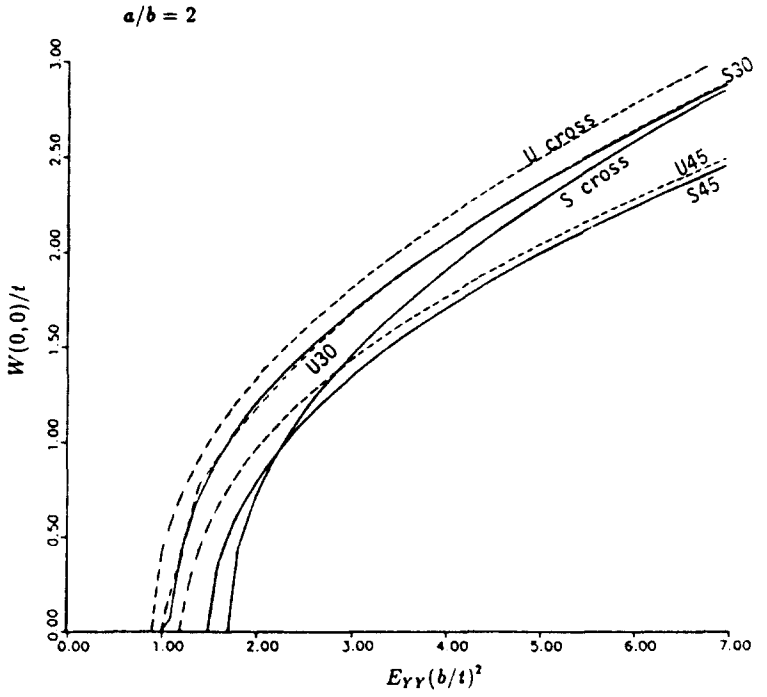

(b)

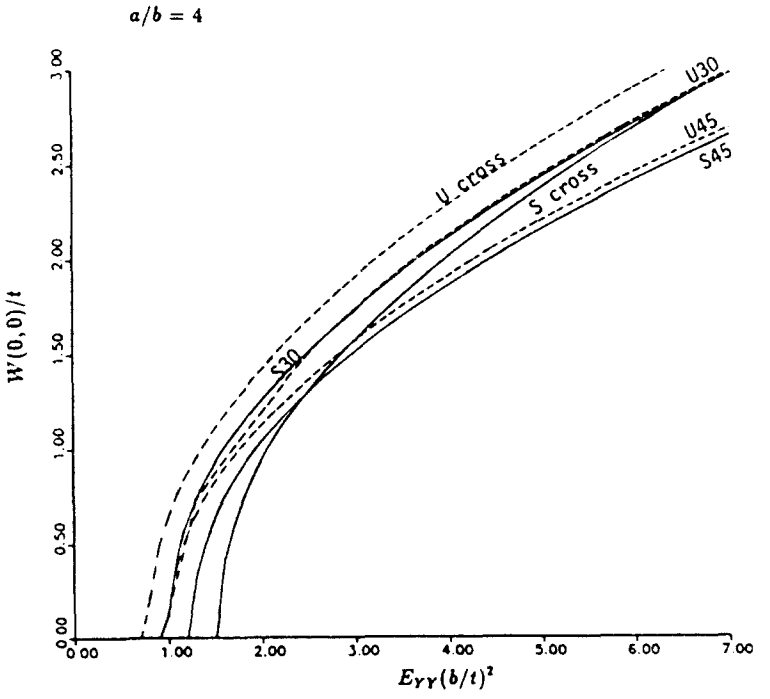

(c)

Fig. 2—*continued.*

3.2. *Membrane forces*

The normal and shearing forces N_{XY} and N_{YY} at the boundary point $(X, Y) = (0, b)$ are shown in Figs 3 and 4. Before buckling, the shearing force vanishes, the normal force is proportional to the applied strain E_{YY} and the results for the sublaminates with symmetric and unsymmetric lay-ups are identical. At the bifurcation strain, the relationship between

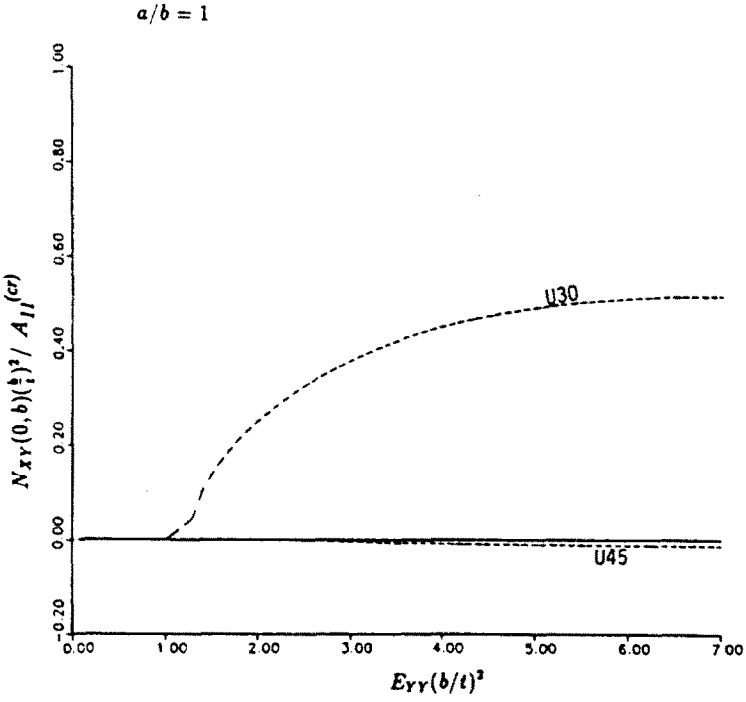

(a)

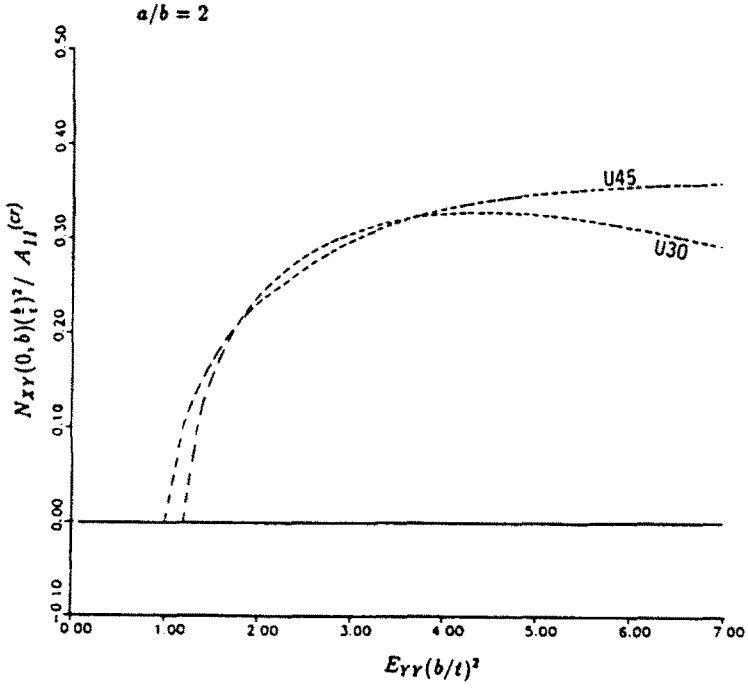

(b)

Fig. 3. N_{YY} at the boundary point $(0, b)$.

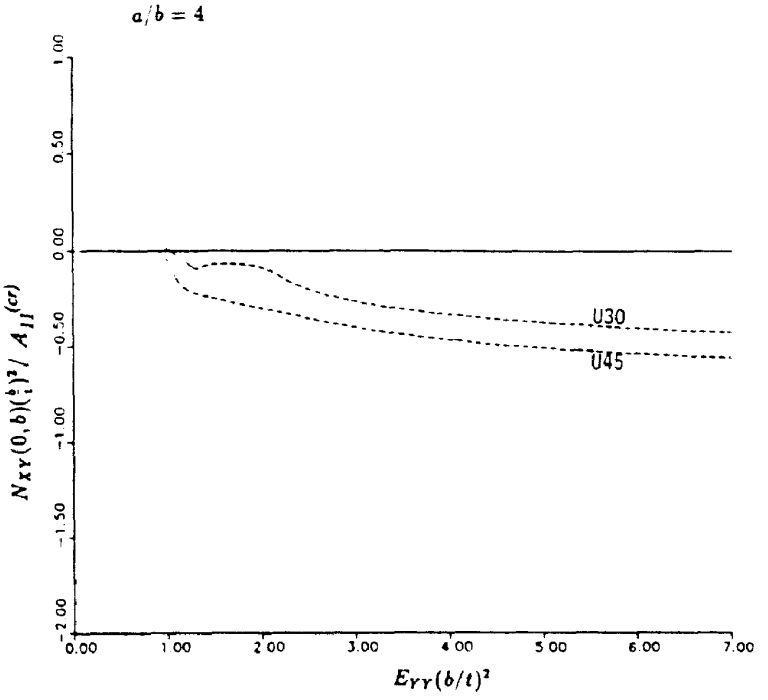

(c)

Fig. 3. *continued.*

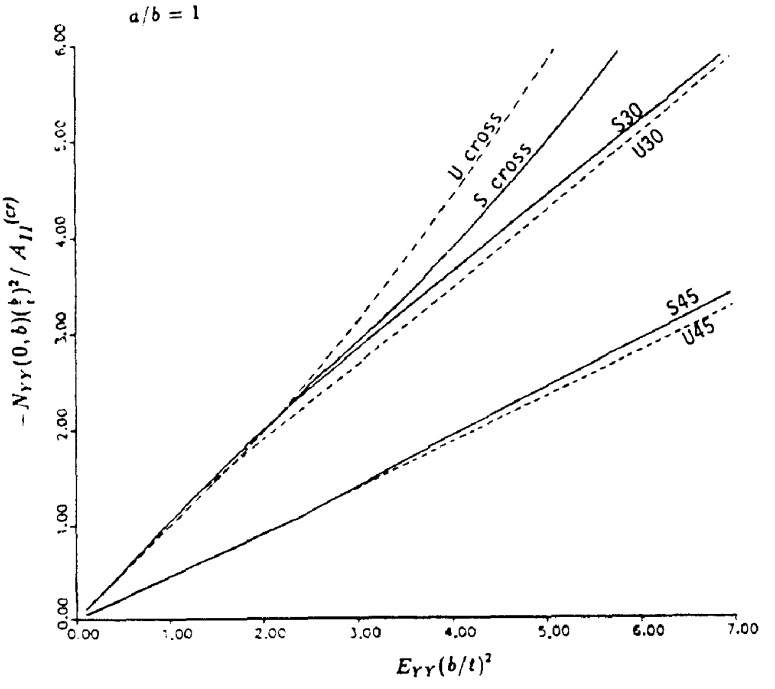

(a)

Fig. 4. N_{YY} at the boundary point $(0, b)$.

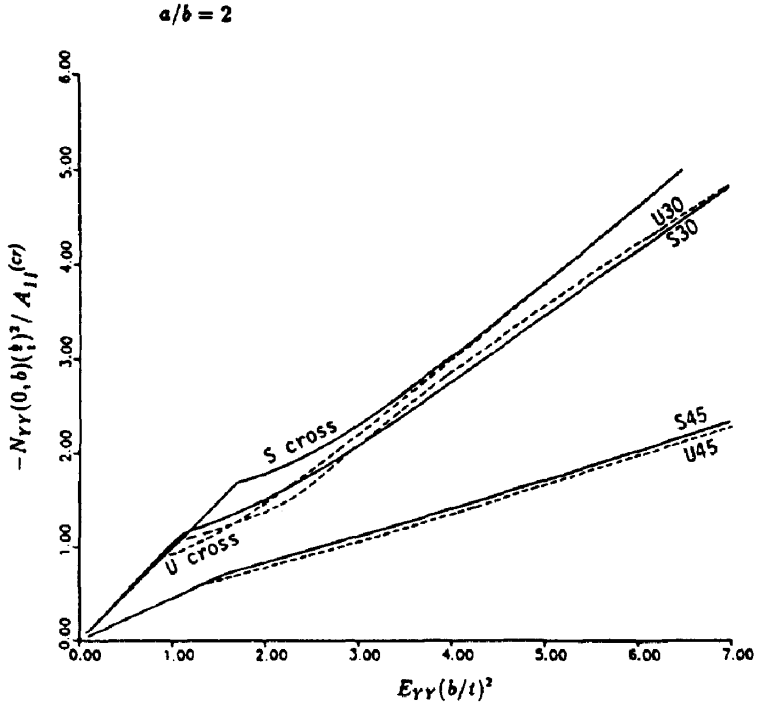

(b)

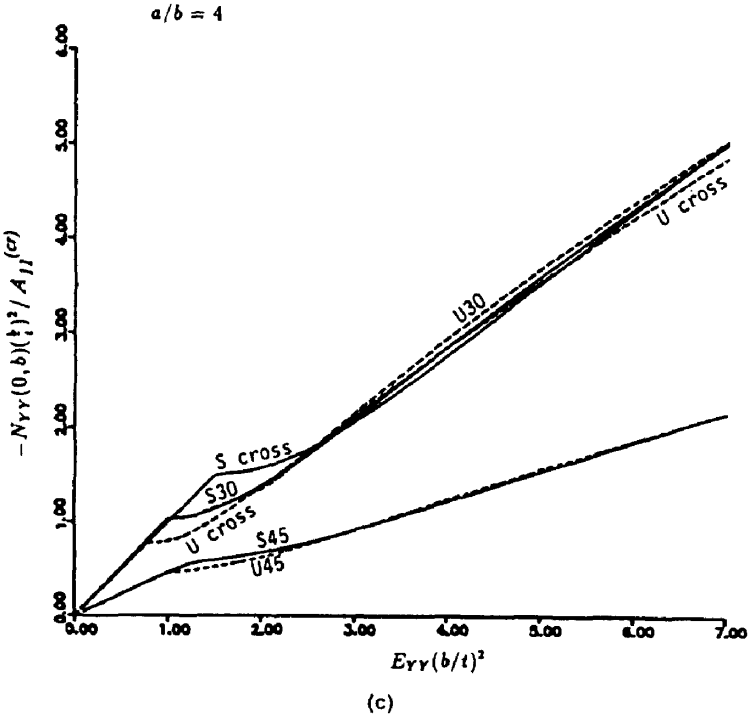

(c)

Fig. 4.—*continued.*

E_{YY} and N_{YY} changes from linear to non-linear. In the cases examined, the larger the aspect ratio a/b, the greater is the deviation from linear relationship in the postbuckling stage. With the exception of the antisymmetric cross-ply circular sublaminate, the deviation of N_{YY} from linear dependence on the postbuckling load is generally on the negative side (i.e. a softening behavior). The postbuckling shearing force N_{XY} is non-zero only for unsymmetric 30° and 45° angle-ply sublaminates, and its values are small compared to the normal force N_{YY} at the same point.

It is interesting to compare the values of N_{YY} at the boundary point $(0, b)$ and at the central point $(0, 0)$. The results at $(0, 0)$, presented in Fig. 5, show much greater deviation from linear dependence on the postbuckling strain load. That is, the decompression in the Y-direction due to sublaminate buckling is greater at the center of the sublaminate and smaller at the two ends of the Y-axis. This is particularly true for the unsymmetric cross-ply sublaminates with aspect ratios 2 and 4, where N_{YY} at $(0, 0)$ changes from compression to tension at an advanced stage of postbuckling. Consequently, the normal force N_{YY} varies significantly from the boundary point $(0, b)$ to the central point $(0, 0)$. A comparison of the results in Fig. 5 yields the rather unexpected observation that the non-uniformity of the in-plane forces tends to be more prominent when the aspect ratio increases from 1 to 2 and finally to 4, i.e. when the geometry of the elliptical delamination becomes more similar to a strip delamination. Although we have not computed the results for elliptical delaminations with even larger aspect ratios, the present results indicate that, as regards the membrane force N_{YY}, there is a significant difference between the postbuckling responses of one-dimensional delaminated layers and of elliptical sublaminates with aspect ratios as large as four. In the first case the axial force is constant whereas in the second case N_{YY} is significantly non-uniform. The non-uniformity of the in-plane forces affects the bending deformation directly, through the bending–stretching coupling of unsymmetrical sublaminates, and indirectly through the strong coupling of in-plane and transverse displacements in the von Karman equations.

Comparison of the transverse in-plane force N_{XX} at the central point and the boundary

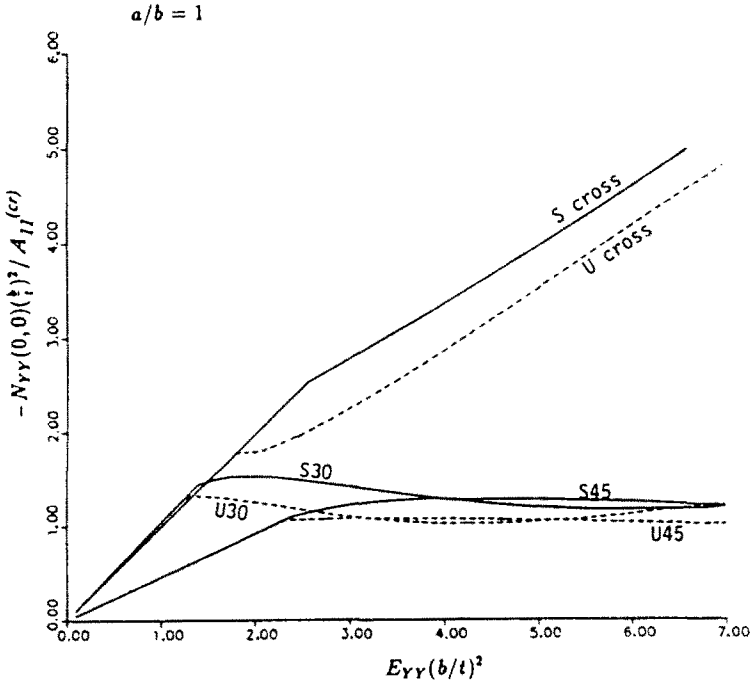

(a)

Fig. 5. N_{YY} at $(0, 0)$.

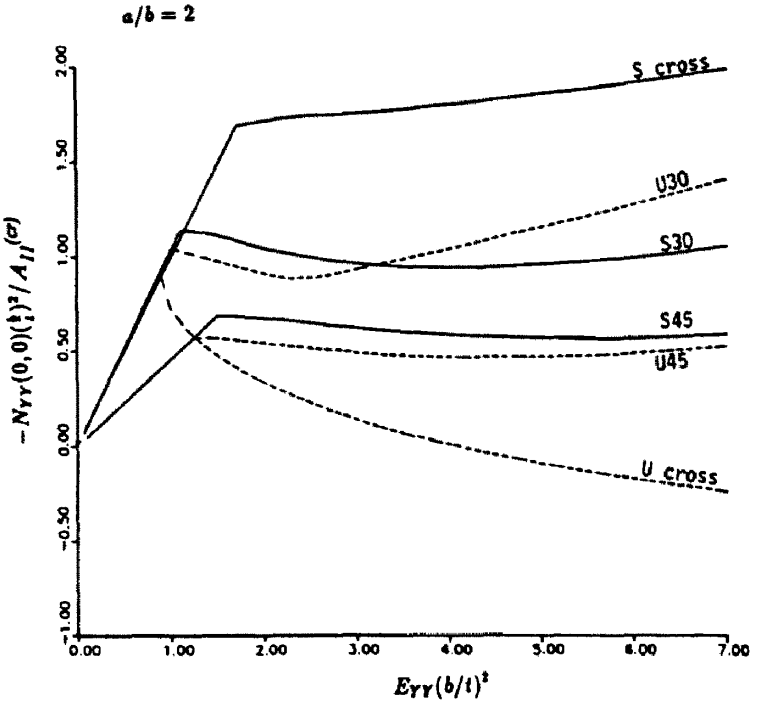

(b)

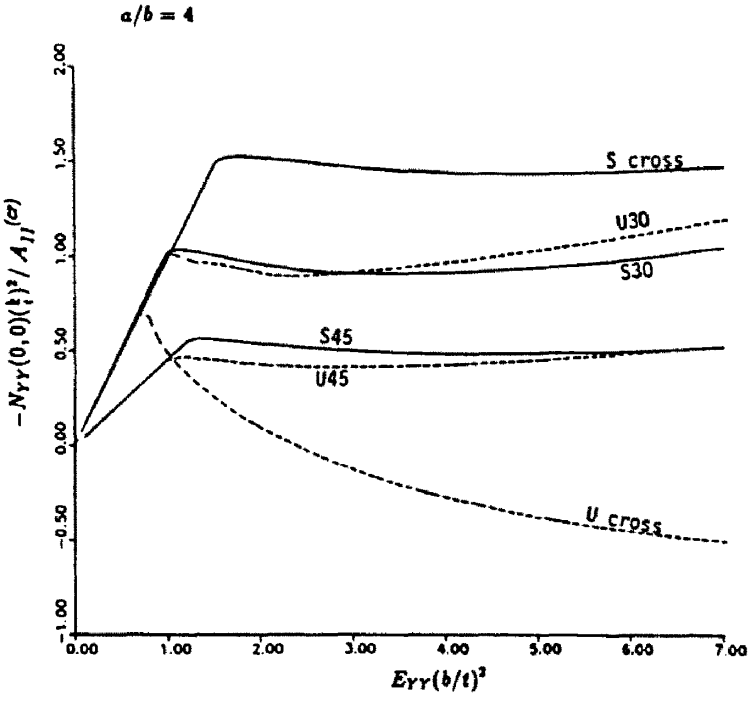

(c)

Fig. 5.—*continued.*

point $(a, 0)$ (shown respectively in Figs 6 and 7) also indicates a significant non-uniformity of that force in the postbuckling stage. Due to the differences of the coupling coefficients in the extensional stiffness matrices, the membrane force N_{xx} in the prebuckling states is tensile for the cross-ply sublaminates and compressive for the 30° and 45° angle-ply sublaminates. For the angle-ply case, the deviation from the linear relationship between N_{xx} and the postbuckling strain load E_{yy} is generally on the positive side (i.e. a hardening behavior), is greater at the central point than at the boundary point $(a, 0)$, and greater for the case of smaller aspect ratio than for the case of larger aspect ratio. However, the unsymmetric cross-ply sublaminates show the almost opposite type of behavior; the postbuckling force N_{xx} in these sublaminates also shows the largest deviation from uniformity.

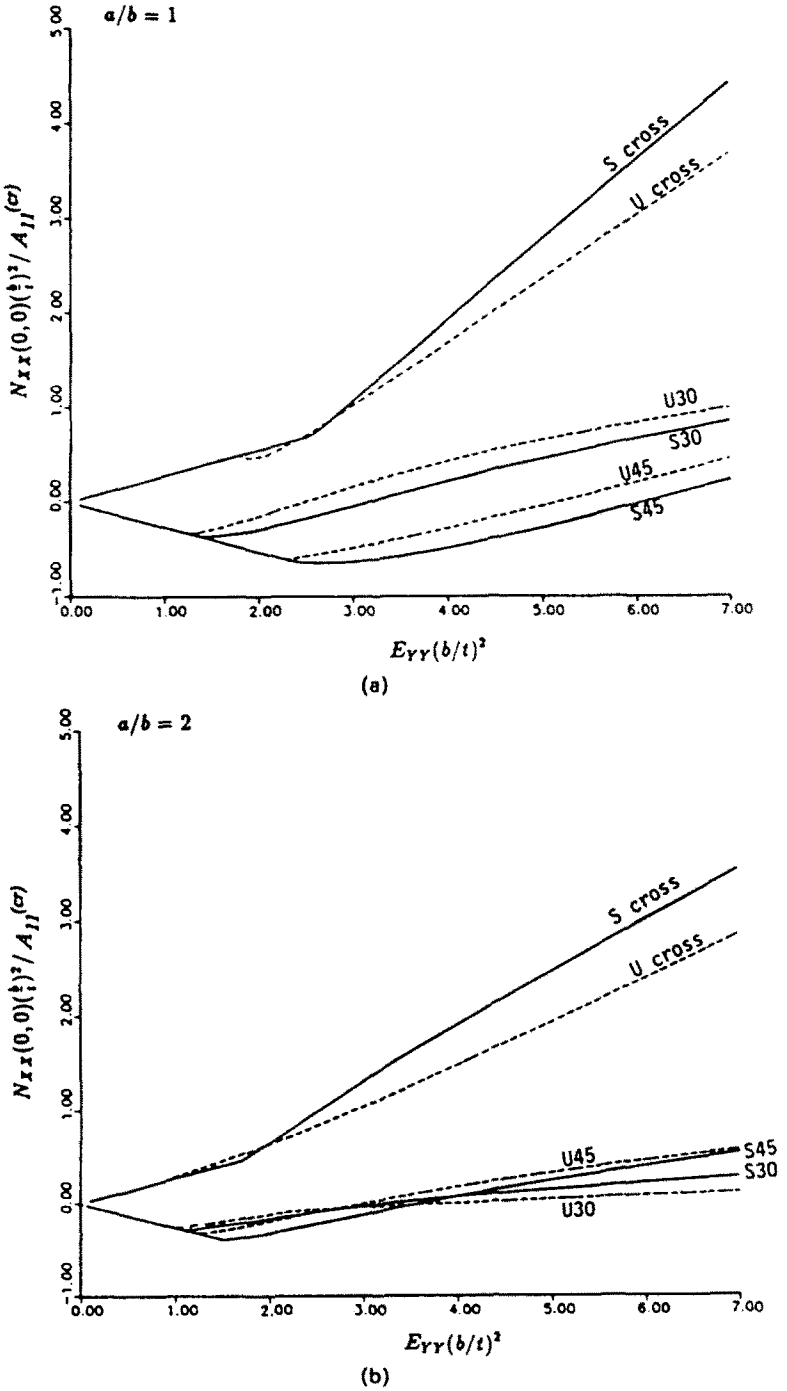

Fig. 6. N_{xx} at (0, 0).

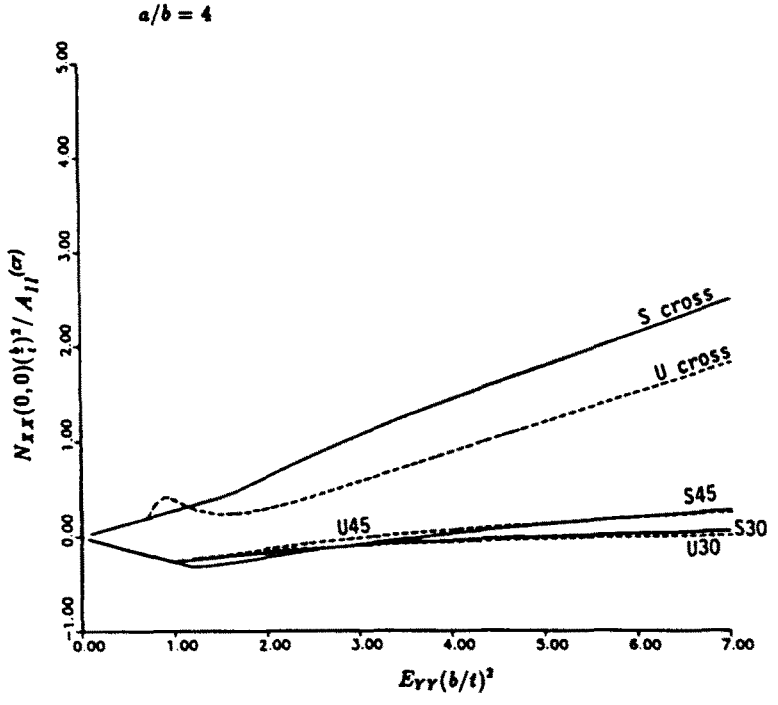

(c)

Fig. 6.—*continued.*

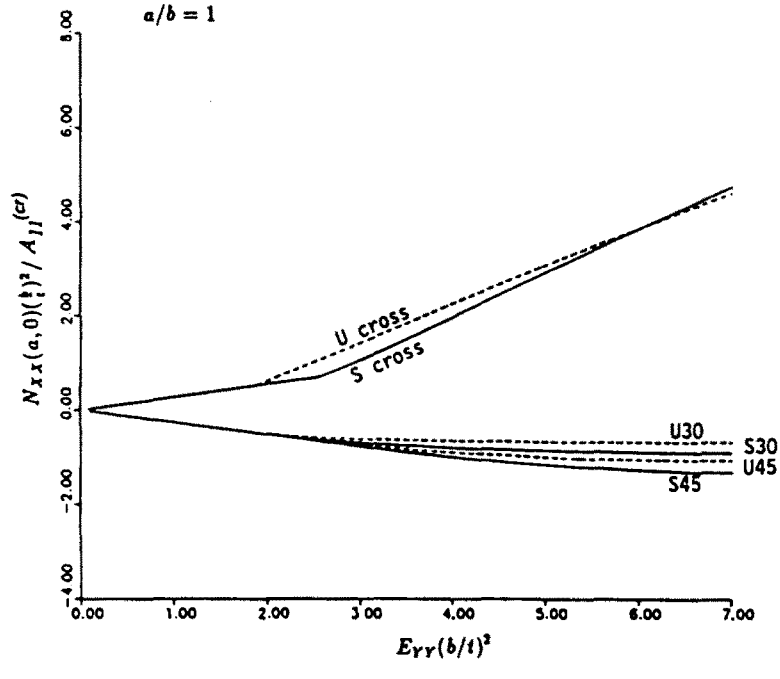

(a)

Fig. 7. N_{xx} at the boundary point $(a, 0)$.

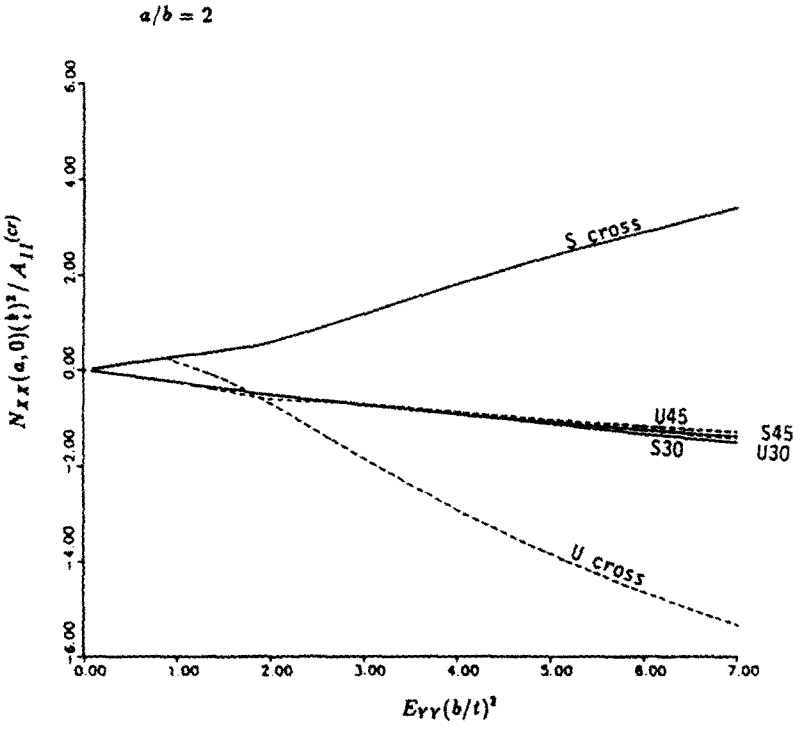

(b)

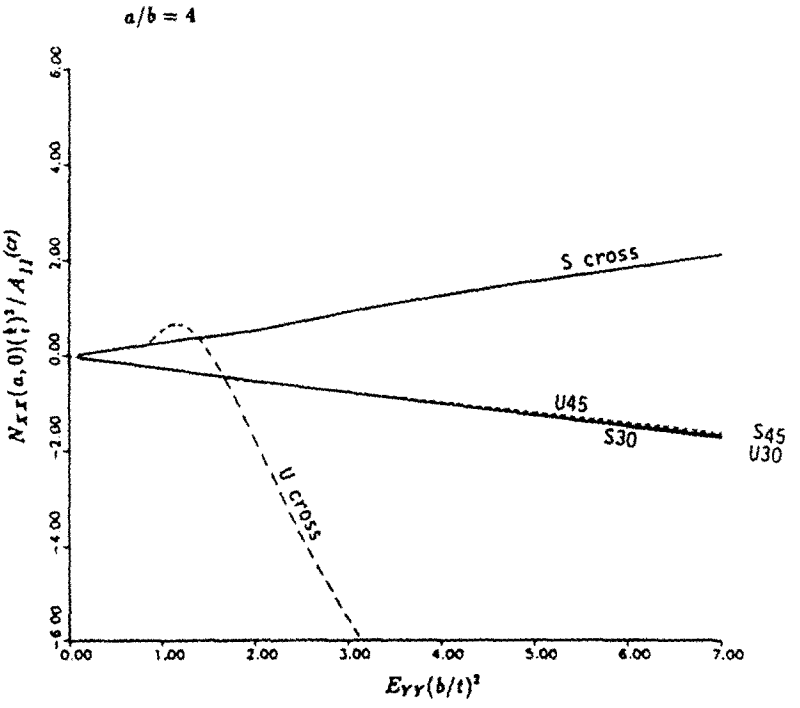

(c)

Fig. 7.—*continued.*

3.3. *Bending and twisting moments; deflection profile*

For all combinations of ply orientation and lay-up, the general behavior of the in-plane forces in the postbuckling stage are remarkably similar between sublaminates with aspect ratios 2 and 4, as may be seen by comparing the respective plots in Figs 2–7. The somewhat different behavior of circular sublaminates is apparently caused by the constraining effect of a relatively short X-axis, as already mentioned before. A similar conclusion holds for the bending moments M_{YY} and M_{XX}. Plots for M_{YY} at $(0, b)$ are shown in Fig. 8 while those for M_{XX} at $(a, 0)$ are shown in Fig. 9. Additional plots for the present

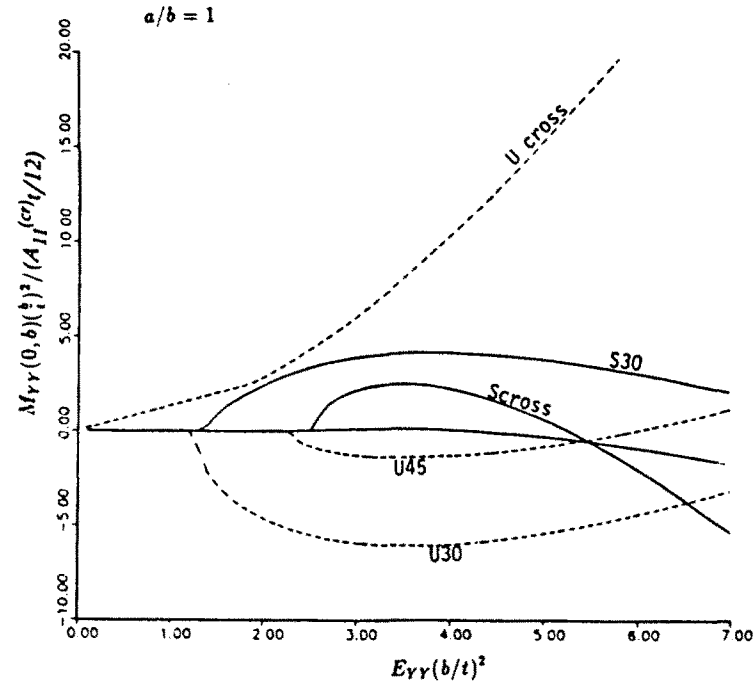

(a)

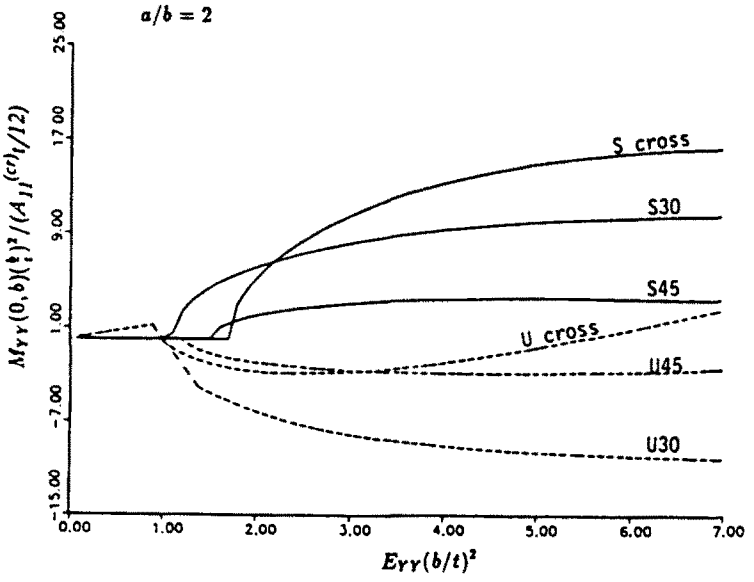

(b)

Fig. 8. Boundary moment M_{YY} at $(0, b)$.

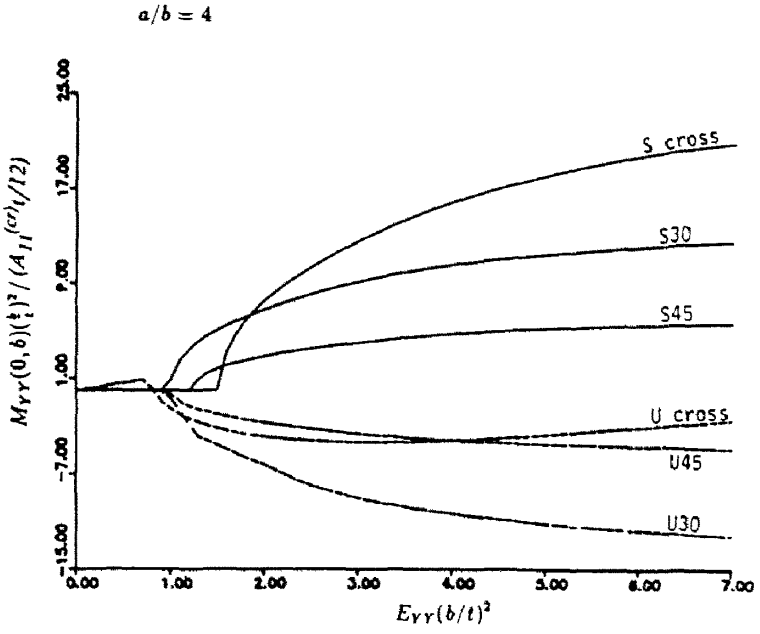

(c)

Fig. 8.—continued.

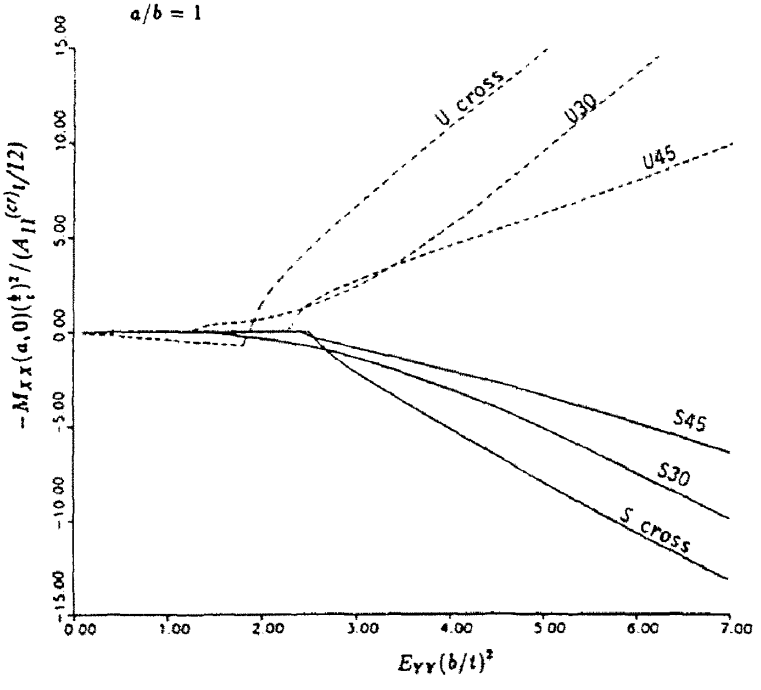

(a)

Fig. 9. Boundary moment M_{XX} at $(a, 0)$.

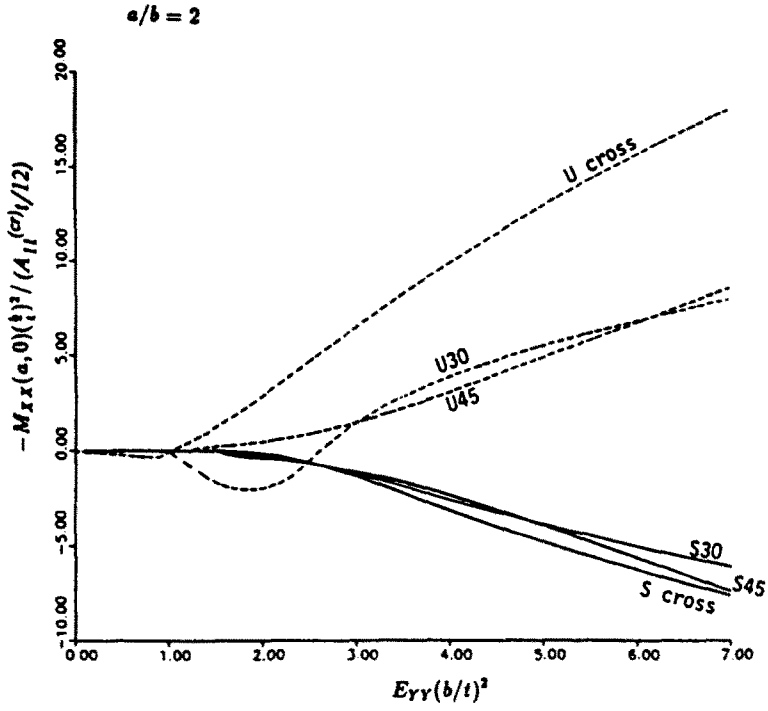

(b)

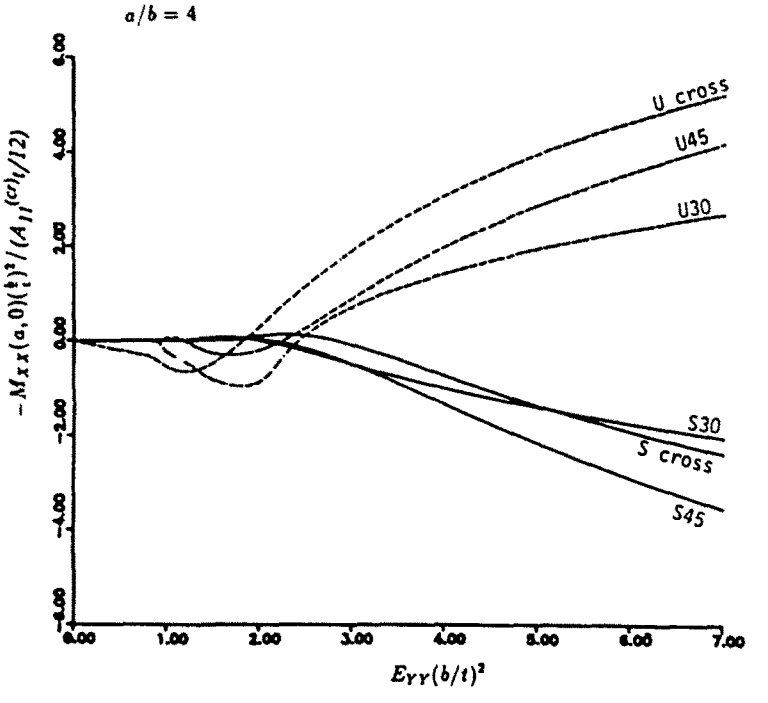

(c)

Fig. 9.—*continued.*

analysis results, including those for the bending moments at the central point $(0, 0)$ may be found in Jane (1989).

The coupling stiffnesses B_{11}, B_{12} and B_{22} vanish in all sublaminates examined in this study except for the unsymmetric cross-ply sublaminate. Hence only the unsymmetric cross-ply sublaminate shows non-zero bending moments M_{XX} and M_{YY} in the prebuckling states. In the postbuckling stage, the relation of the bending moments to the strain load is very complex. However, for sublaminates with aspect ratios 2 and 4, the bending moment M_{YY} at the boundary point $(0, b)$ is generally much greater, in absolute value, than the corresponding moment at the central point. For sublaminates with aspect ratios 1 and 2, the bending moment M_{XX} at $(a, 0)$ is also much greater, in absolute value, than the corresponding moment at $(0, 0)$. For $a/b = 4$, the bending moment M_{XX} at $(a, 0)$ is not large, because a relatively large curvature of the clamped boundary curve at that point provides a restraining effect on the transverse deflection in the vicinity.

In the absence of strong bending–stretching coupling, the bending moment is largely determined by the curvature of the deformed sublaminate. The profiles of the deformed middle surface are shown in Figs 10 and 11 for cross-ply and 45° angle-ply sublaminates under a normalized strain of $-E_{YY}(b/t)^2 = 3$, and in Fig. 12 for 30° angle-ply sublaminates under a normalized strain of 2.0. The left and right portions of the figures indicate the profiles along the Y-axis and the X-axis, respectively. The solid curves refer to the sublaminates with symmetric lay-ups, while the dashed curves refer to those with unsymmetric lay-ups. It is seen that, along the X-axis, the curvature of the profile attains much larger absolute values in the vicinity of the boundary point $(a, 0)$ than around the central point. In contrast, along the Y-axis the curvature of the profile attains relatively small absolute values at the boundary point $(0, b)$ compared to the central point.

Since the curvature of the deformed middle surface of the plate directly affects the normal bending moment at a boundary point, which in turn contributes significantly to an opening action of the delaminated layer from the base laminate (provided that the boundary curvature is positive so that the deflection is non-negative), the concentration of the normal curvature near the boundary point $(a, 0)$, and its attenuation near the point $(0, b)$, tend to

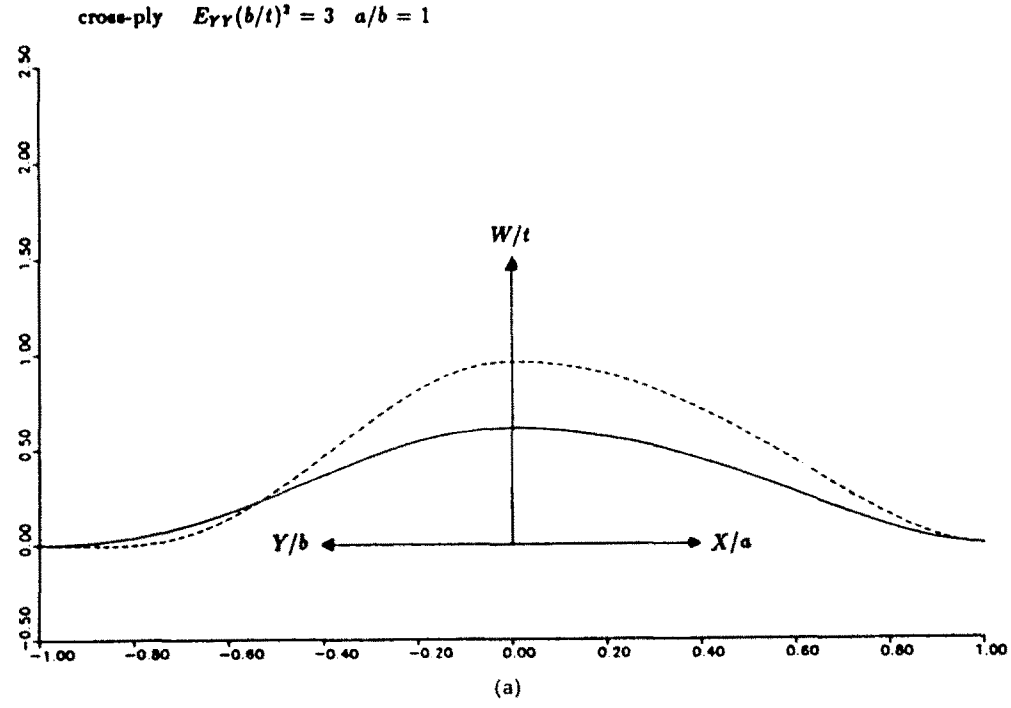

(a)

Fig. 10. Deflection profiles of cross-ply laminates (normalized strain load = 3.0).

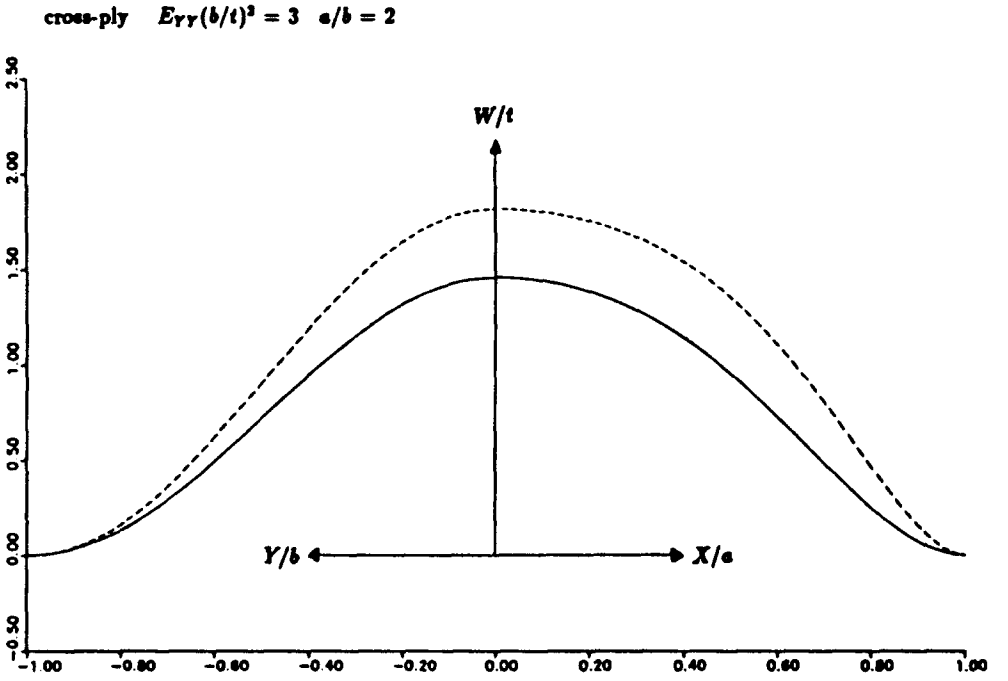

(b)

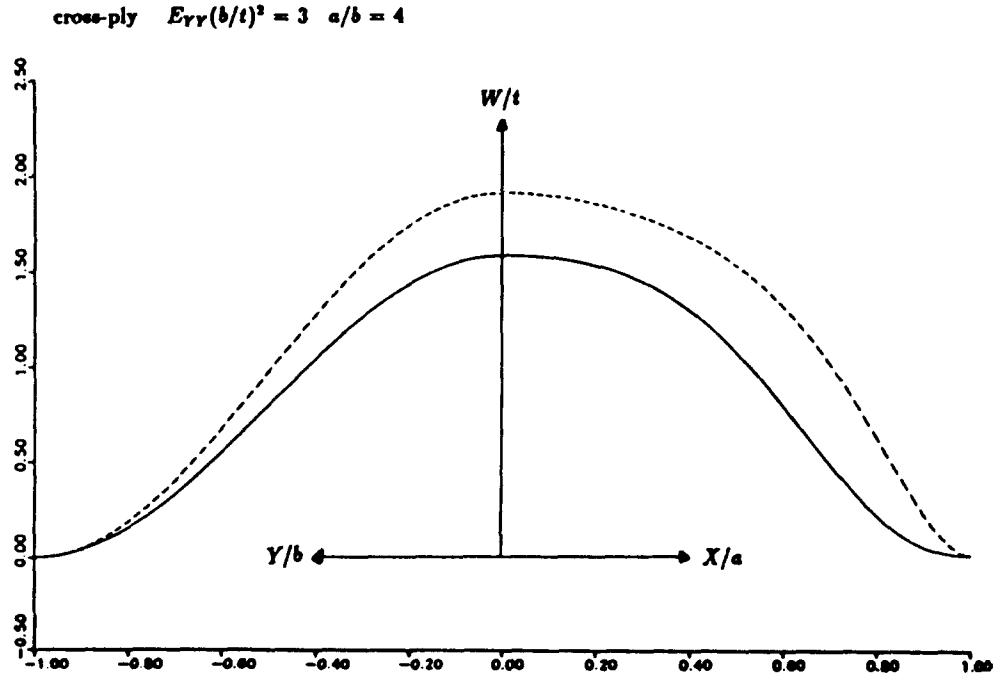

(c)

Fig. 10.—*continued.*

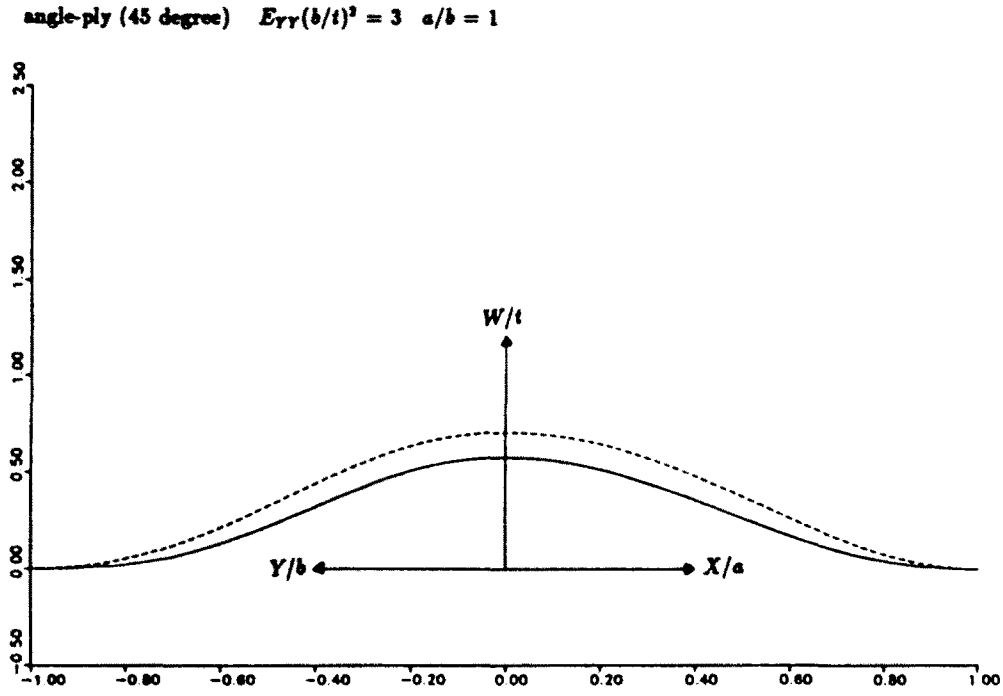

(a)

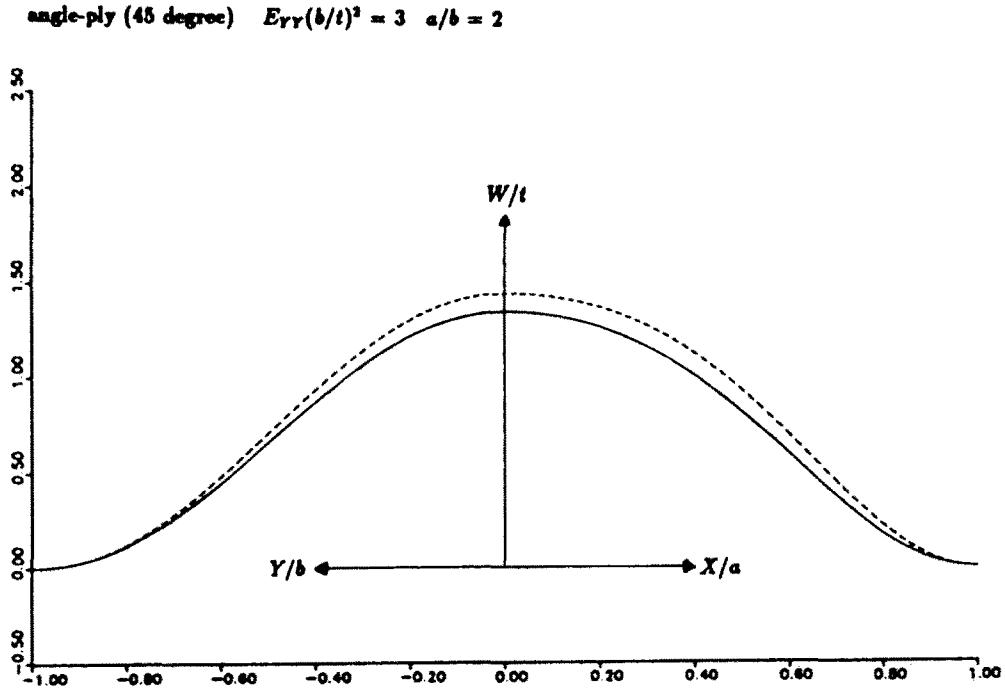

(b)

Fig. 11. Deflection profiles of 45° angle-ply laminates (normalized strain load = 3.0).

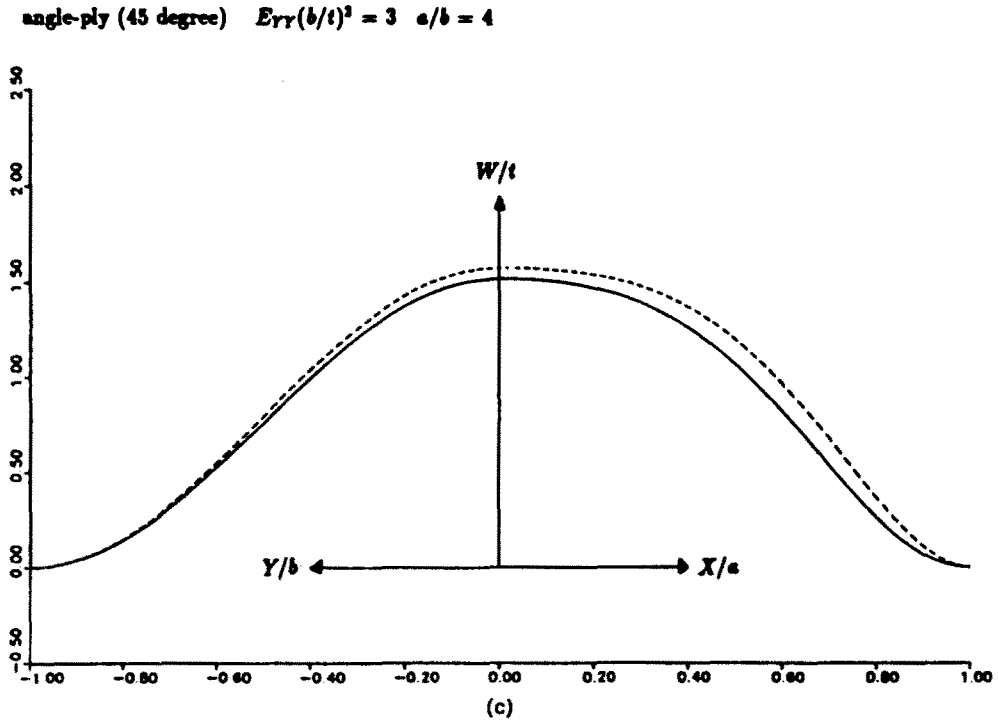

(c)

Fig. 11.—*continued.*

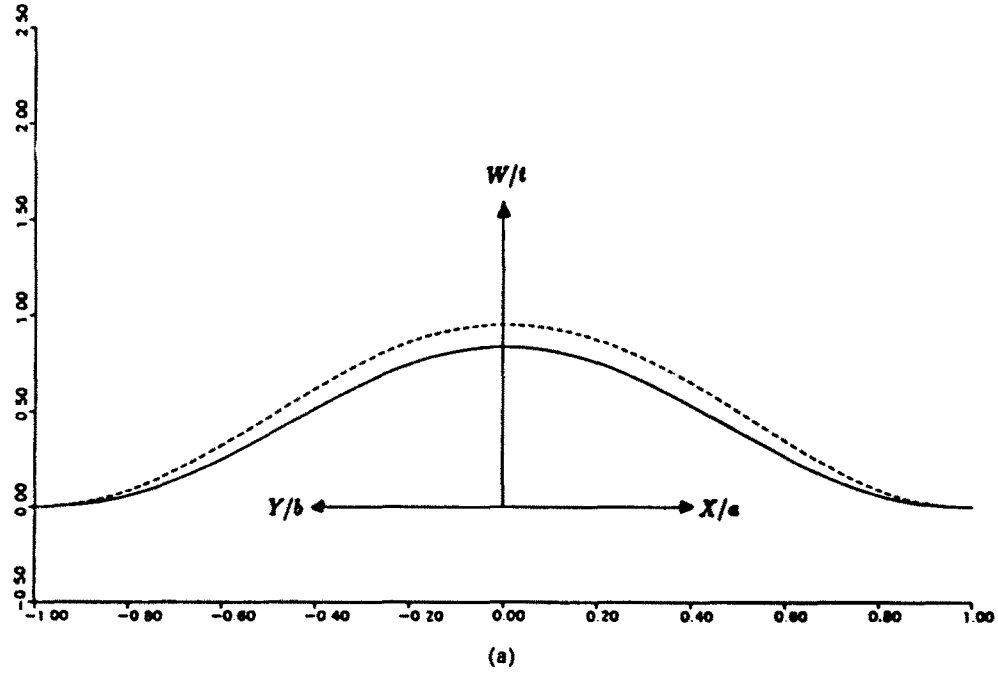

(a)

Fig. 12. Deflection profiles of 30° angle-ply laminates (normalized strain load = 2.0).

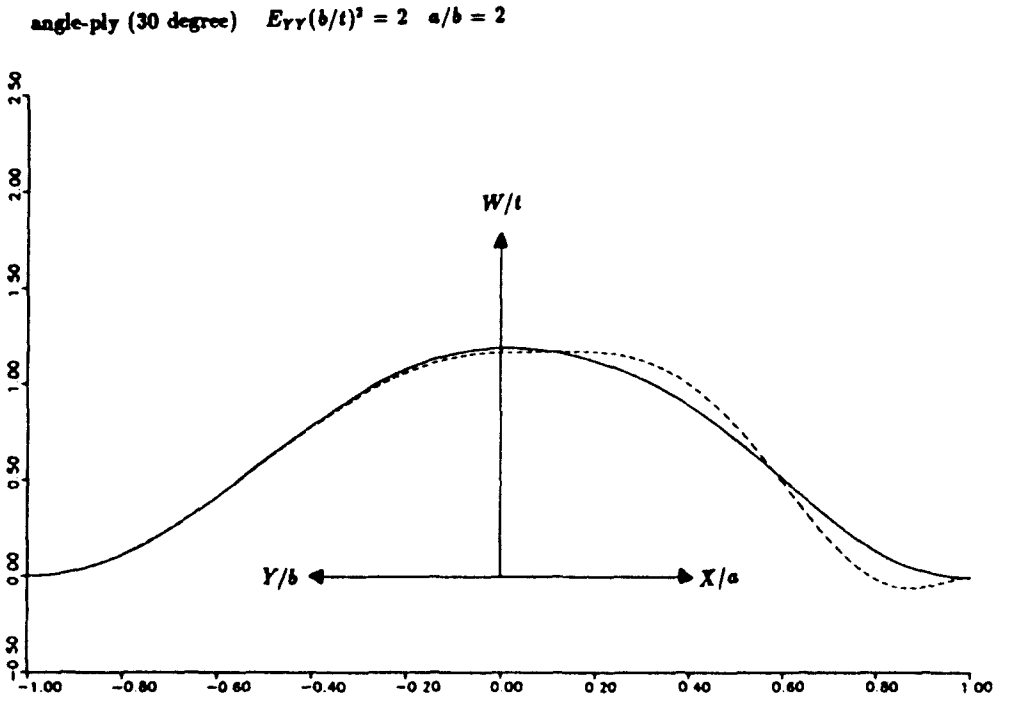

(b)

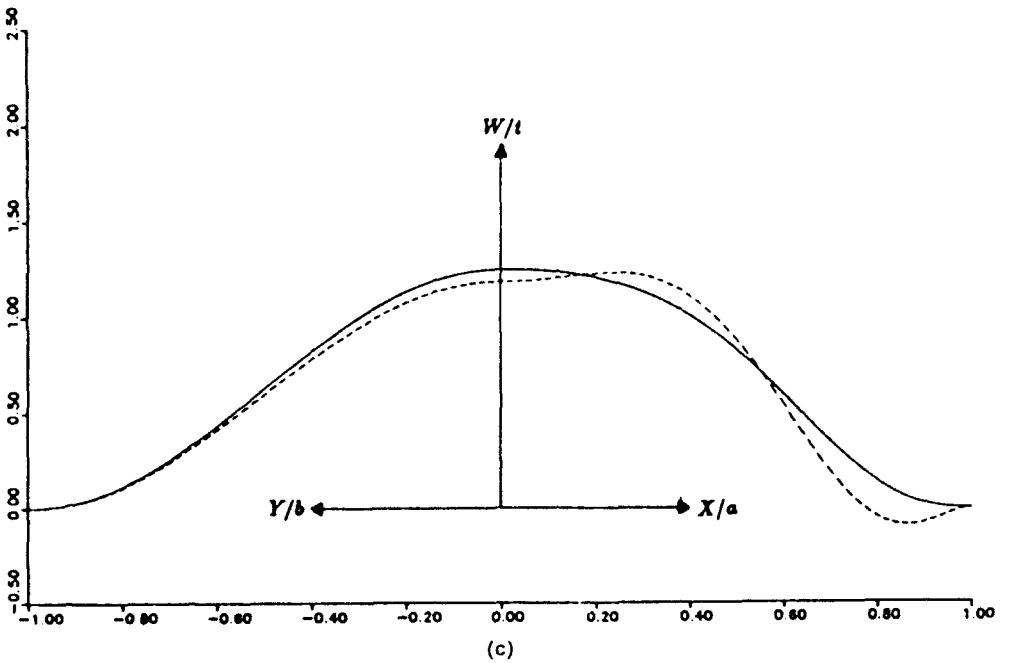

(c)

Fig. 12.—*continued.*

facilitate the growth of the delamination along the X-direction, i.e. the direction perpendicular to that of the compressive loading axis. However, this conclusion is only valid when the aspect ratio is not large. When the growth of the delamination in the transverse direction results in a sufficiently large a/b, the normal curvature at $(a, 0)$ becomes small relative to that at $(0, b)$, because of the longer length of the X-axis in the profiles.

It is interesting to note that the postbuckling deflections of the unsymmetric 30° angle-ply sublaminates with aspect ratios 2 and 4 show multiple wave patterns in the X-direction (see the second and third figures in Fig. 12). This is perhaps essentially due to the relatively small bending stiffness of such sublaminates in the X-direction. Furthermore, these solutions show negative deflection in the vicinity of the boundary point $(a, 0)$ while the solutions of unsymmetric cross-ply sublaminates with $a/b = 1$ show negative deflection near the boundary point $(0, b)$. Since negative deflections imply partial contact of the sublaminate with the base laminate, such mathematical solutions must be modified to take account of the contact condition. However, this difficult task is not attempted in the present work.

The deflection profiles of the 45° angle-ply sublaminates are similar to those of the cross-ply sublaminates with the same aspect ratio. However, the results for sublaminates with symmetric and unsymmetric lay-ups are closer in the 45° case than in the cross-ply case, because the bending–stretching coupling effect in unsymmetric sublaminates is relatively small in the former case compared to the latter case. Furthermore, local contact between the sublaminate and the base plate does not occur in the postbuckling deformation of 45° angle-ply sublaminates for any one of the three aspect ratios.

3.4. *Global and pointwise energy release rates*

For thin-film delaminates with a general shape, the energy-release rate at each point of the delamination boundary may be evaluated in terms of the normal and shearing in-plane forces and the normal bending moment and the twisting moment at that boundary point. The results for the pointwise energy release rates at the two boundary points $(a, 0)$ and $(0, b)$ are shown in Figs 13 and 14, respectively, in terms of the imposed strain load. As the imposed strain increases, the energy release rate at $(a, 0)$ grows more rapidly for the delaminations with smaller a/b, although the bifurcation strains for such delaminations are

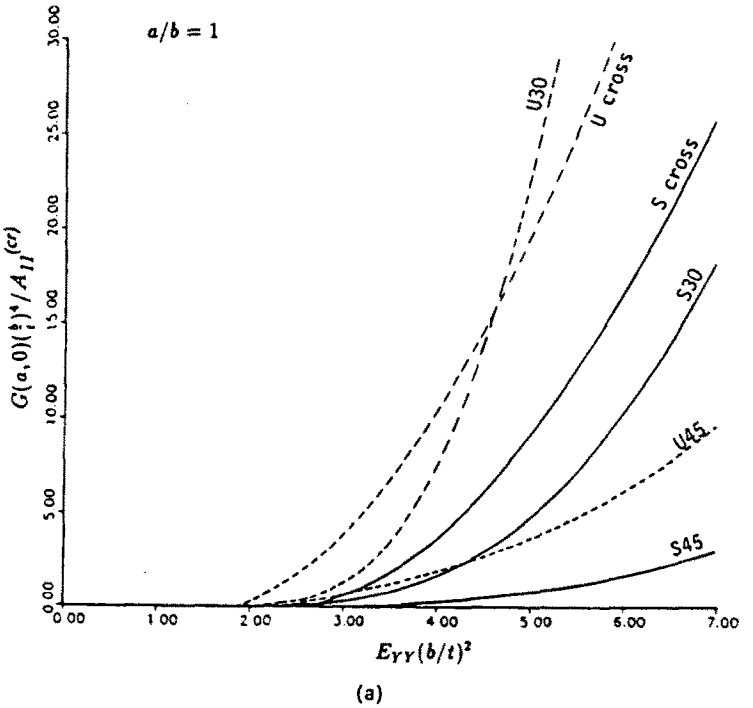

(a)

Fig. 13. Strain-energy release rate at $(a, 0)$.

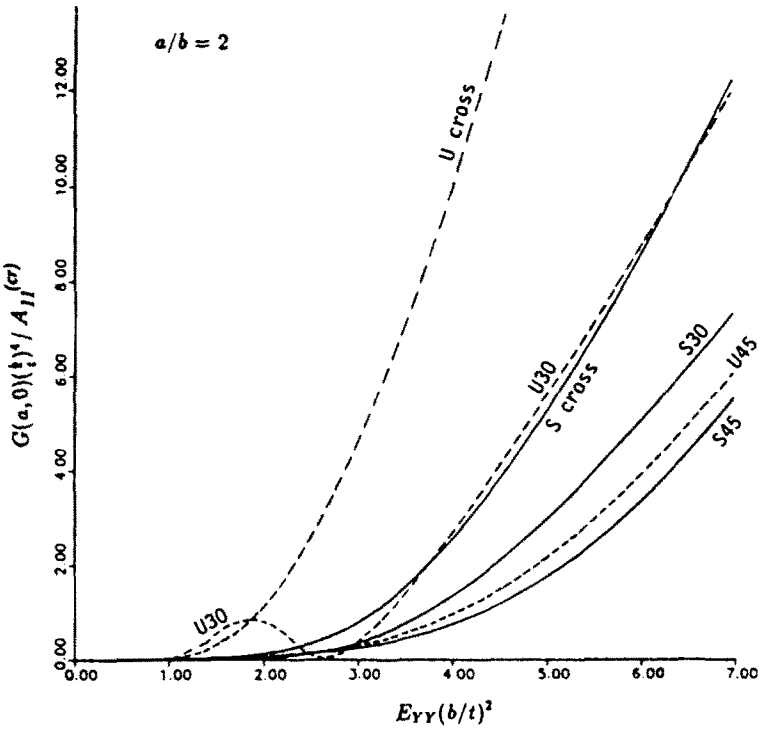

(b)

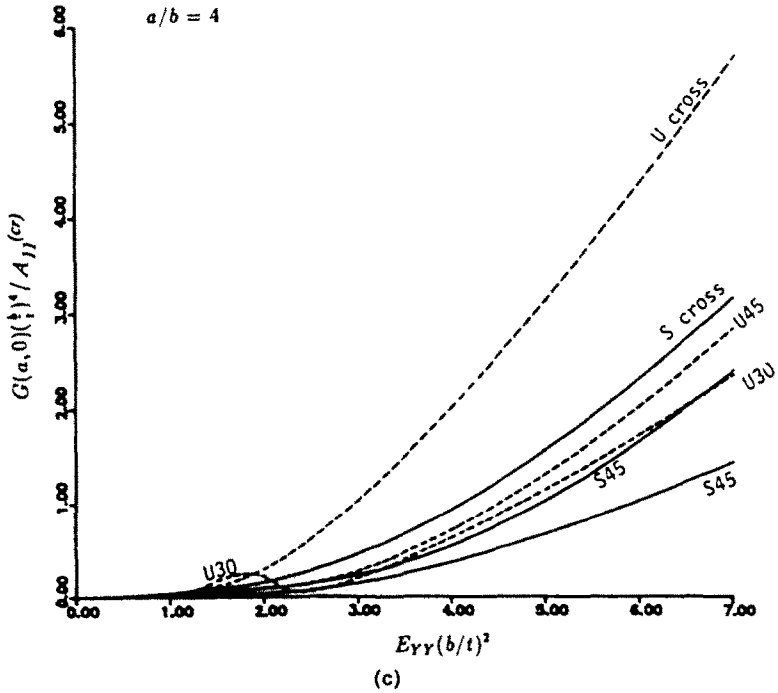

(c)

Fig. 13.—*continued.*

greater. In contrast, the energy release rate at $(0, b)$ grows more rapidly, in general, for delaminations with larger a/b. For the circular delamination, the value at $(a, 0)$ dominates over the value at $(0, b)$. If the pointwise energy release rate is used as the criterion of delamination growth, then for a delamination model with a near circular initial shape subjected to an increasing compressive load along the Y-axis, postbuckling delamination growth tends to proceed first along the X-axis until the aspect ratio becomes sufficiently large so that the local energy release rates at $(a, 0)$ and $(0, b)$ become equalized. Afterwards, stable delamination growth may continue under an increasing load in such a manner that the energy release rates at all points of the moving delamination boundary are equal, i.e. equal to the critical value for growth. In unstable, dynamic delamination growth, the local energy release rates at different points of the moving boundary need not be equal because the growth criterion may depend on the crack moving speed.

It should be mentioned that, in case of anisotropic elliptical sublaminates, the maximum and minimum values of the boundary forces and moments and of the energy release rates generally do not occur at the point $(a, 0)$ or $(0, b)$. Consequently, postbuckling growth of an initially elliptical delamination generally proceeds in such a manner that the shape of the delamination becomes non-elliptical. Therefore, a procedure for predicting the delamination growth behavior based on evaluating the *global* energy release rates associated with growth along fixed co-ordinate directions is generally not applicable to two-dimensional delaminations in an anisotropic base plate. In such a procedure, the global energy release rates are obtained for an *assumed* manner of growth by evaluating the potential energies of the delamination model in two successive states of growth and by differentiating the results numerically with respect to the increasing semi-axial lengths of the ellipse. These global energy release rates are fundamentally different from the pointwise energy release rates used in the present study. Indeed, as shown by the present results, their relation to the strain load is very much different from that of the pointwise energy release rates. In cases where the consideration of global energy release rate may be justified, the use of the pointwise and global energy release rates are likely to yield somewhat different predictions with regard to the delamination growth behavior.

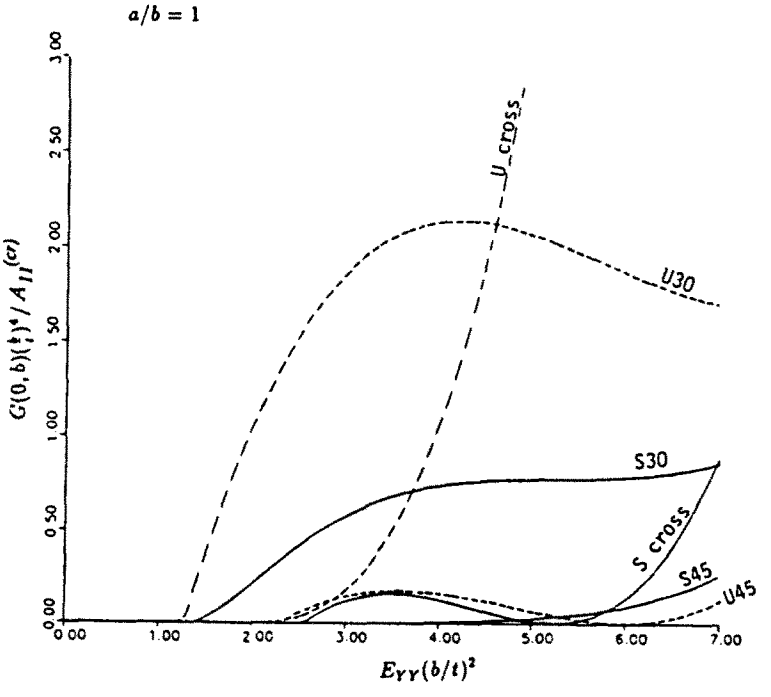

(a)

Fig. 14. Strain-energy release rate at $(0, b)$.

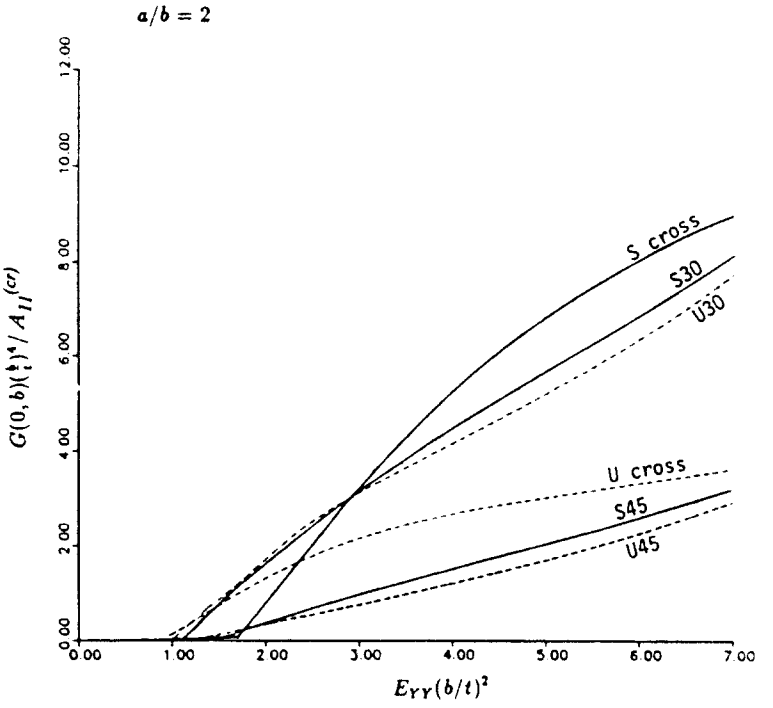

(b)

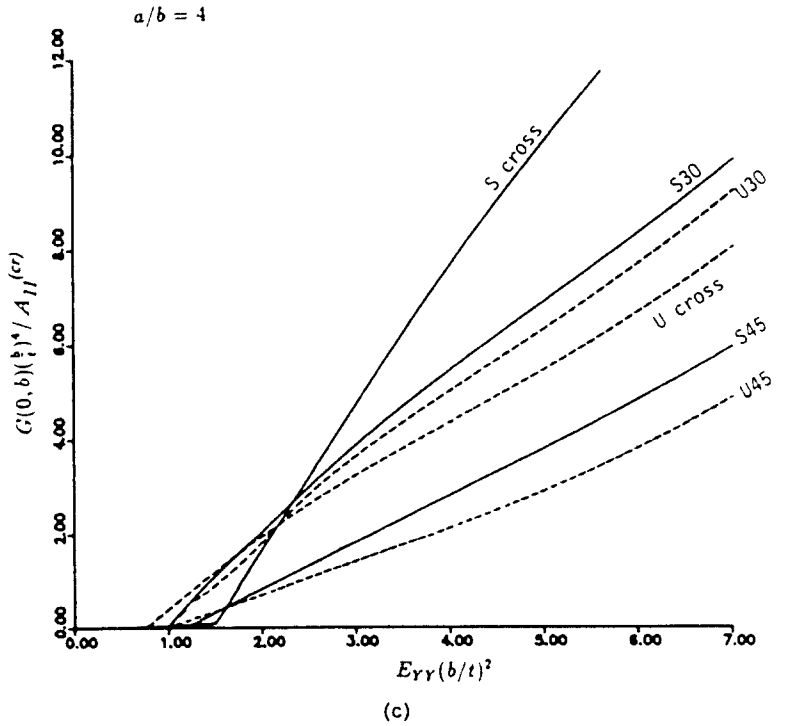

(c)

Fig. 14.—*continued.*

4. CONCLUSIONS AND ADDITIONAL REMARKS

Several conclusions with far-reaching implications for the analysis and understanding of sublaminate buckling and crack growth associated with two-dimensional models may be drawn from the results of the present study. Some of these conclusions have been suggested in previous publications (Yin, 1989; Storakers, 1989). They are substantiated, in the present work, by examining Rayleigh–Ritz postbuckling solutions of elliptical sublaminates and by comparing solutions of the various orders.

(1) The bifurcation loads of thin-film elliptical delaminations may be calculated accurately by a Rayleigh–Ritz analysis involving a small number of undetermined coefficients. The results are better than those obtained by alternative methods [for example, Woinowsky-Krieger (1937) and Kassapoglou (1988)].

(2) The postbuckling behavior of a strip delamination model is rather exceptional because the non-linear von Karman equations reduce to a *linear* ordinary differential equation in the case of plane strain buckling. The solutions of strip models do not show non-uniformity of the in-plane deformation in the sublaminate and concentration of curvature of the deformed middle surface around boundary regions. These effects are significant and have important implications on the postbuckling and growth behavior of two-dimensional delamination models.

(3) The non-linear and boundary effects mentioned above cannot be determined, or determined with sufficient accuracy, by a linearized postbuckling analysis or by a Rayleigh–Ritz analysis involving lower-order polynomial expansions of the displacements. Predictions of the force and moment resultants in the sublaminate and of the delamination growth behavior based on Rayleigh–Ritz solutions of order lower than (5, 4) are generally unreliable.

(4) As the orders of polynomials in the displacement expansions increase, the deflection, forces, moments and energy release rates associated with the Rayleigh–Ritz solutions of circular delaminations in axisymmetric deformation converge towards the corresponding results obtained by direct integration of the von Karman equations (Yin, 1985). The convergence confirms the validity of the latter solution, whose results are significantly different to the solution obtained by the perturbation method (Bottega and Maewal, 1983). Rayleigh–Ritz solutions of the order (5, 4) deliver good results over a range of strain loads up to about three times the bifurcation strain. Solutions of the order (7, 6) yield better results over a much wider range of the strain load. On the other hand, solutions of the order (5, 6) are nearly indistinguishable from those of the order (5, 4). The results suggest that higher degree polynomials should be used in the expansions of the in-plane displacements so as to allow adequate modeling of the non-uniformity of the in-plane deformation.

(5) The computational effort involved in solving the non-linear algebraic equations associated with the Rayleigh–Ritz method is small compared to solving the same problem by non-linear finite-element modeling since the number of degrees of freedom required in the latter method may be considerably larger. In implementing the Rayleigh–Ritz method, the major task consists of algebraic manipulations and integrations for obtaining the potential energy function. Given specific polynomial expansions of the displacements, this task needs to be performed only once in obtaining the functions L_{ij}, M_{ij} and N_{ij} (see eqn (6) in Part I of this paper). When these functions are determined, the potential energy functions and the governing algebraic equations for elliptical delaminations with different thicknesses, aspect ratios and stiffness matrices may be obtained in a straightforward manner. Consequently, the Rayleigh–Ritz method is ideally suited for a parametric study of the postbuckling behavior of elliptical laminates with diverse geometrical and material configurations.

A recent study of buckling, postbuckling and failure of elliptical delaminations has appeared which is also based on the perturbation method (Kassapoglou, 1988). While the work does not present sufficiently detailed results on postbuckling deformation to make a comparison with the present solutions feasible, it yields bifurcation loads with relatively

large errors (several percent). Generally speaking, any method of analysis which fails to provide very accurate results for the bifurcation load cannot be expected to yield acceptable results for the postbuckling deformation, because the buckling problem is a linearized problem whereas the postbuckling problem is strongly non-linear. It therefore appears that, unless higher-order perturbed equations are used, the perturbation method is not a promising approach for obtaining accurate solutions beyond an initial stage of postbuckling deformation.

In selecting the order of Rayleigh–Ritz solutions used in the present study we have taken into account the limitation on the validity of the solutions imposed by the thin-film assumption and the omission of the transverse shear effect. Polynomial expansions of the displacements are truncated at the order where further improvement in the accuracy of the solutions is believed to be within the error caused by these two assumptions. Recently, the effect of transverse shear deformation on the buckling and postbuckling behavior has been studied for strip delamination models (Kardomateas and Schmueser, 1988; Chen, 1990) and thin-film elliptical sublaminates (Peck, 1989). The results depend essentially on the slenderness of the delaminated layer and the base plate. Analytical solutions for strip delamination models, obtained by the use of a shear correction factor, indicate that the transverse shear effect may appreciably reduce the buckling load and significantly increase the energy release rate under a given postbuckling axial load.

Peck (1989) used a higher-order laminated plate theory in conjunction with the Rayleigh–Ritz method to calculate the buckling loads and postbuckling solutions of elliptical sublaminates. This provides a better approach to the assessment of the transverse shear effect in laminated plates than the use of a single shear correction factor (independent of the elastic anisotropy, orientation and lay-up of the constituent plies). It should be mentioned, however, that since the significance of the transverse shear effect increases with the thickness of the sublaminate, the effect may be more important in the delaminated portion of the base plate than in a thin delaminated layer. Hence an adequate evaluation of the transverse shear effect in delamination problems may require a complete analysis of the delamination model without using the thin-film assumption.

Acknowledgement—The completion of this work was made possible by a grant from U.S. Army Research Office to Georgia Institute of Technology. The authors gratefully acknowledge the support.

REFERENCES

Bottega, W. J. and Maewal, A. (1983). Delamination buckling and growth in laminates. *J. Appl. Mech.* **50**, 184–189.

Chai, H. and Babcock, C. D. (1985). Two-dimensional modelling of compressive failure in delaminated laminates. *J. Comp. Mater.* **19**, 67–98.

Chai, H., Babcock, C. D. and Knauss, W. G. (1981). One dimensional modelling of failure in laminated plates by delamination buckling. *Int. J. Solids Structures* **17**, 1069–1083.

Chen, H.-P. (1990). A variational principle consistent shear deformation theory on compressive delamination buckling and growth. *Proc. AIAA/ASME/ASCE/AHS/ASC 31st SDM Conference*, Long Beach, CA, 1208–1217.

Jane, K. C. (1989). Buckling, postbuckling deformation and vibration of a delaminated plate. Ph.D. Thesis, Georgia Institute of Technology, Atlanta, GA.

Kardomateas, G. A. (1989). Large deformation effects in the postbuckling behavior of composites with thin delamination. *AIAA Jl* **27**, 624–631.

Kardomateas, G. A. and Schmueser, D. W. (1988). Buckling and postbuckling of delaminated composites under compressive loads including transverse shear effects. *AIAA Jl* **26**, 337–343.

Kassapoglou, C. (1988). Buckling, post-buckling and failure of elliptical delaminations in laminates under compression. *Comp. Struct.* **9**, 139–159.

Peck, S. O. (1989). Compressive behavior of delaminated composite plates. Ph.D. Thesis, Stanford University, Palo Alto, CA.

Shivakumar, K. N. and Whitcomb, J. D. (1985). Buckling of a sublaminate in a quasi-isotropic composite laminate. *J. Comp. Mater.* **19**, 2–18.

Simitses, G. J., Sallam, S. N. and Yin, W.-L. (1985). Effect of delamination of axially loaded homogeneous laminated plates. *AIAA Jl* **23**, 1437–1444.

Storakers, B. (1989). Nonlinear aspects of delamination in structural members. In *Theoretical Mechanics, Proc. XVIIth Int. Congr. Theor. Appl. Mech.* (Edited by P. Germain, M. Piau and D. Caillerie), pp. 315–336. Elsevier, New York.

Woinowsky-Krieger, S. (1937). The stability of a clamped elliptical plate under uniform compression. *J. Appl. Mech.* **4**, 177–178.

Yin, W.-L. (1985). Axisymmetric buckling and growth of a circular delamination in a compressed laminate. *Int. J. Solids Structures* **21**, 503–514.

Yin, W.-L. (1986). Cylindrical buckling of laminated and delaminated plates. *Proc. AIAA ASME ASCE/AHS 27th SDM Conference*, San Antonio, Texas, 165–179.

Yin, W.-L. (1988). The effects of laminated structure on delamination buckling and growth. *J. Comp. Mater.* **22**, 502–517.

Yin, W.-L. (1989). Recent analytical results in delamination buckling and growth. In *Interlaminar Fracture in Composites* (Edited by A. E. Armanios), pp. 253–266. Trans Tec., Switzerland.

Yin, W.-L. and Fei, Z. (1984). Buckling load of a circular plate with a concentric delamination. *Mech. Res. Comm.* **11**, 337–344.

Yin, W.-L. and Fei, Z. (1988). Delamination buckling and growth in a clamped circular plate. *AIAA Jl* **26**, 438–445.

Yin, W.-L., Sallam, S. N. and Simitses, G. J. (1986). Ultimate axial load capacity of a delaminated beam-plate. *AIAA Jl* **24**, 123–128.